Supplementary Information

Ni-N-C catalyst for CO_2 electroreduction based on MOF@MOF configuration exhibiting wide active reaction sites

Chul Hyun Jun[a], Chandan Chandru Gudal[a], Sampath Prabhakaran[b], Anki Reddy Mule[a], Pil J. Yoo[a], Do Hwan Kim[c], Chan-Hwa Chung*[a]*

[a] *School of Chemical Engineering, Sungkyunkwan University (SKKU), Suwon 16419, Republic of Korea*

[b] *Department of Nano Convergence Engineering (BK21 FOUR), Jeonbuk National University, Jeonju, Jeonbuk, 54896, Republic of Korea*

[c] *Division of Science Education, Department of Energy Storage/Conversion Engineering (BK21 FOUR), Jeonbuk National University, Jeonju, Jeonbuk, 54896, Republic of Korea*

*dhk201@jbnu.ac.kr, chchung@skku.edu

Computational calculation method

Spin-polarized DFT calculations were conducted using the Vienna ab initio simulation package,[1,2] employing a projector-augmented Plane-wave pseudopotential with a cutoff energy of 400 eV for valence electrons. The generalized gradient approximation, specifically the Perdew–Burke–Ernzerhof (PBE) form, was utilized for exchange–correlation potentials.[3,4] To account for van der Waals interaction, the DFT-D3 method proposed by Grimme was applied to correct dispersion forces.[5] The simulations were performed on a two-dimensional layer with vacuum regions extending approximately 16 Å along Z-directions to prevent interaction between layers. For optimization, the Brillouin zone was sampled by 4 × 4 × 1.

The adsorption energy (E_{ad}) for the adsorbate on the catalyst is expressed by the formula $E_{ad} = E_{ads/cat} - E_{ads} - E_{cat}$, where $E_{ads/cat}$ represents the total energy of the slab with the adsorbate, E_{ads} is the energy of an adsorbed molecule, and E_{cat} is the energy of the clean catalyst substrate. The calculation of the Gibbs free energy change (ΔG) was performed for the reaction mechanism outlined in equations (1)-(3).[6]

$$CO_2(g) + * + H^+ + e^- \leftrightarrow *COOH \qquad \Delta G_1 \qquad (1)$$

$$*COOH + H^+(aq) + e^- \leftrightarrow *CO + H_2O \qquad \Delta G_2 \qquad (2)$$

$$*CO \leftrightarrow CO(g) + * \qquad \Delta G_3 \qquad (3)$$

The * denotes the active site on the substrate, while *COOH and *CO signify intermediate species adsorbed on the active sites of the catalyst. Electrochemical reduction of CO_2 can lead to a various range of products. The Gibbs free energy change for the adsorption of the molecule was computed using the equation (4):[5]

$$\Delta G_{ads*} = E_{ads/cat} - E_{ads} - E_* + \Delta E_{ZPE} - T\Delta S \qquad (4)$$

where ΔE_{ZPE} and ΔS are the vibrational zero-point energy change and the entropy change, respectively. ΔG_1, ΔG_2, and ΔG_3 are Gibbs free energy changes in each reaction step.

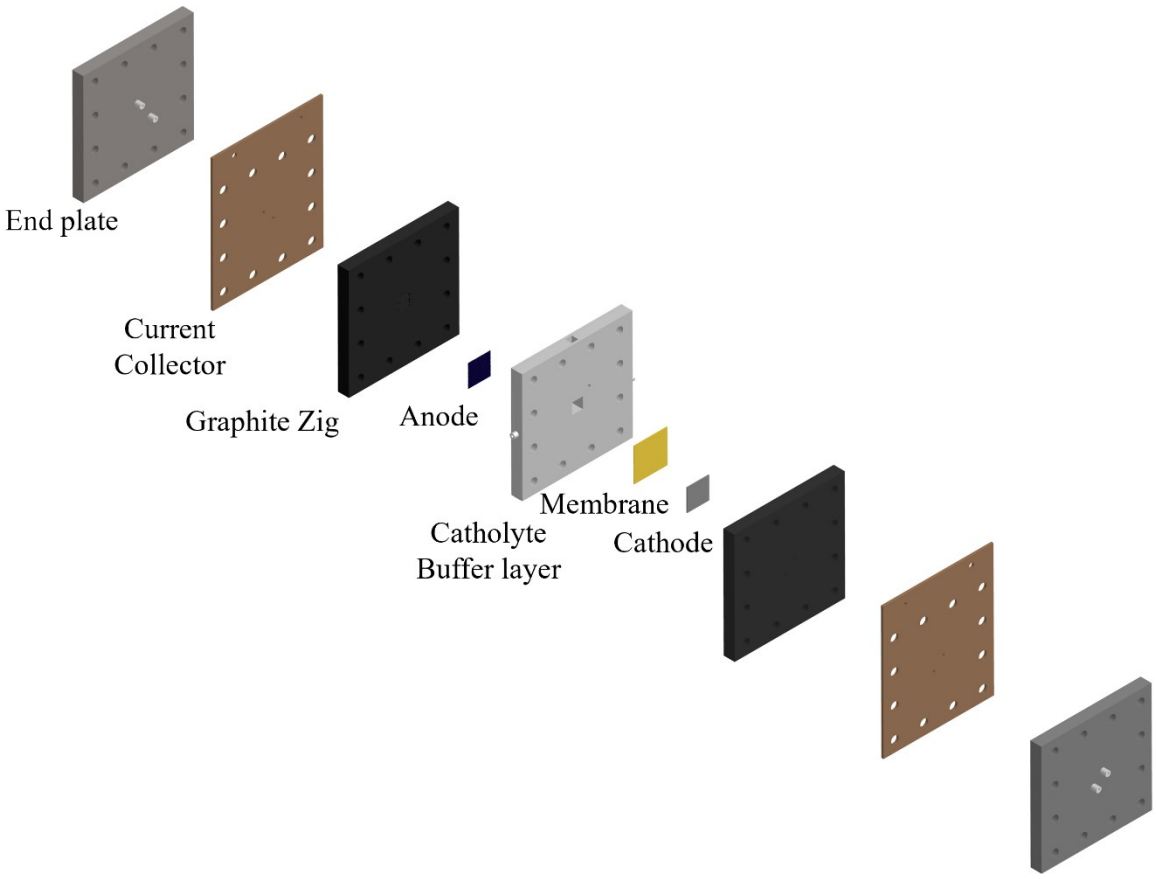

Fig. S1. Schematic diagram of a flow cell.

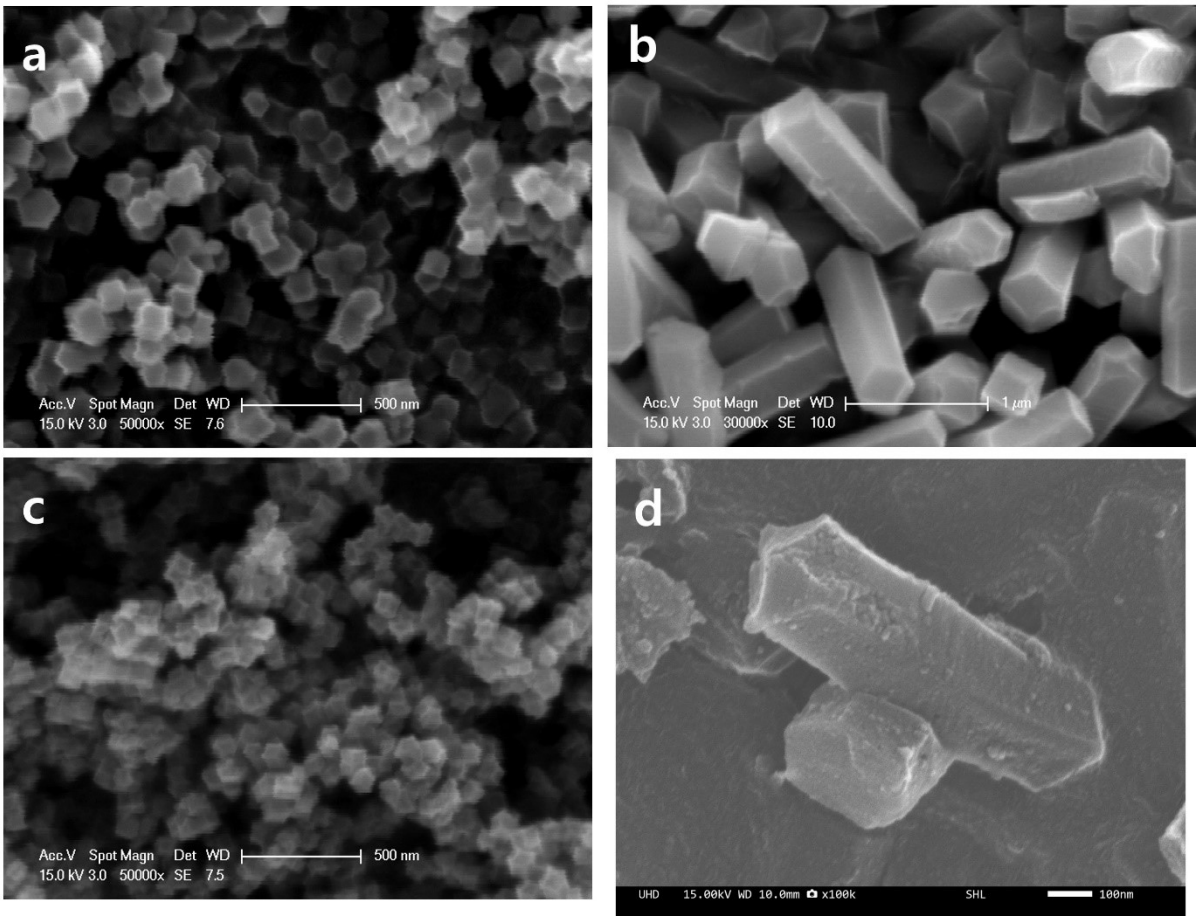

Fig. S2. SEM images of a) ZIF-8(Ni), b) MOF-74, c) Ni-N-C-8 and d) P-MOF-74.

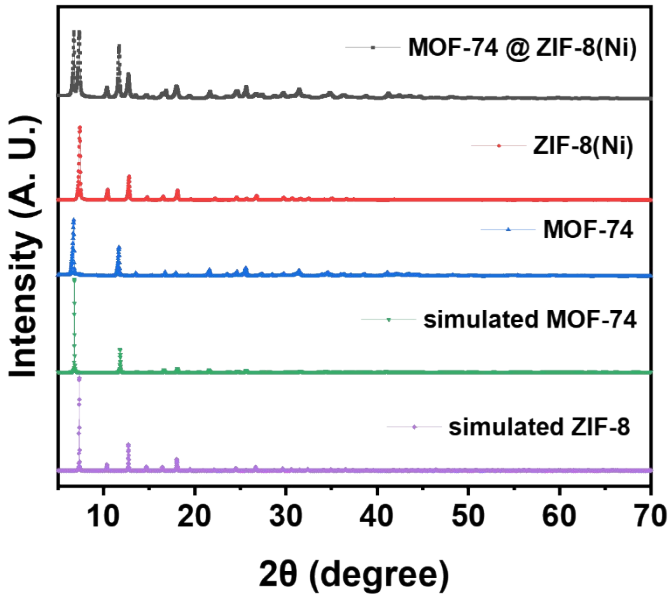

Fig. S3. XRD spectra of MOF-74@ ZIF-8(Ni), ZIF-8(Ni), MOF-74, simulated MOF-74 and simulated ZIF-8.

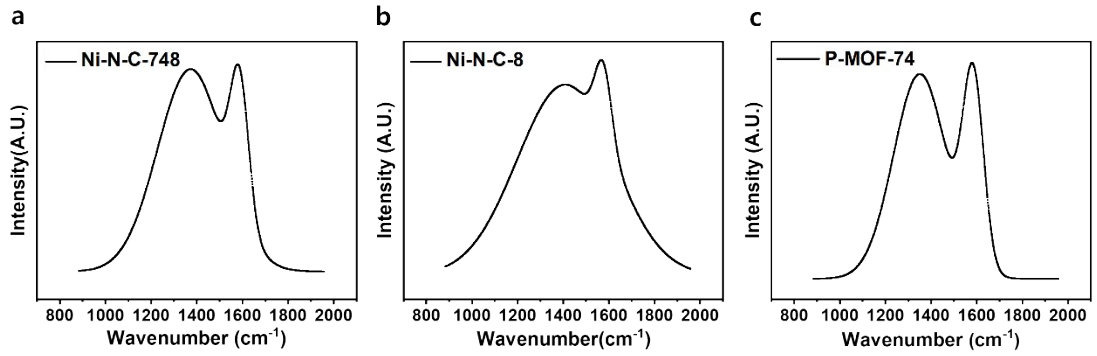

Fig. S4. Raman spectra of a) Ni-N-C-748, b) Ni-N-C-8 and c) P-MOF-74.

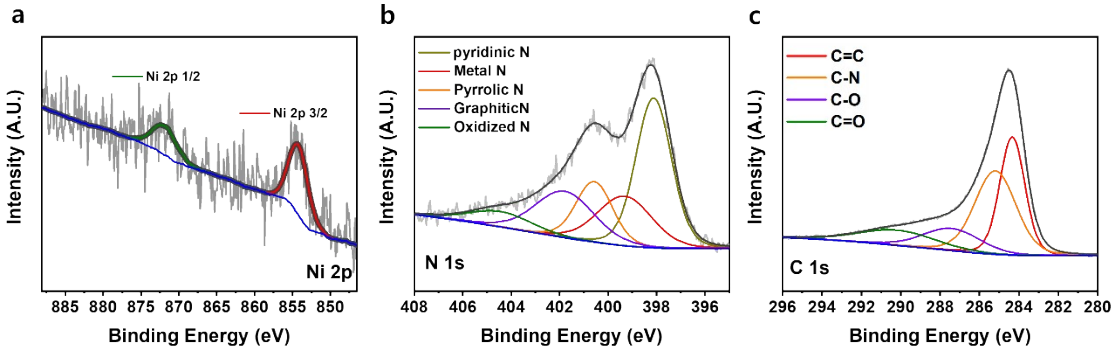

Fig. S5. a) Ni 2p, b) N 1s, and c) C 1s XPS spectra of Ni-N-C-8.

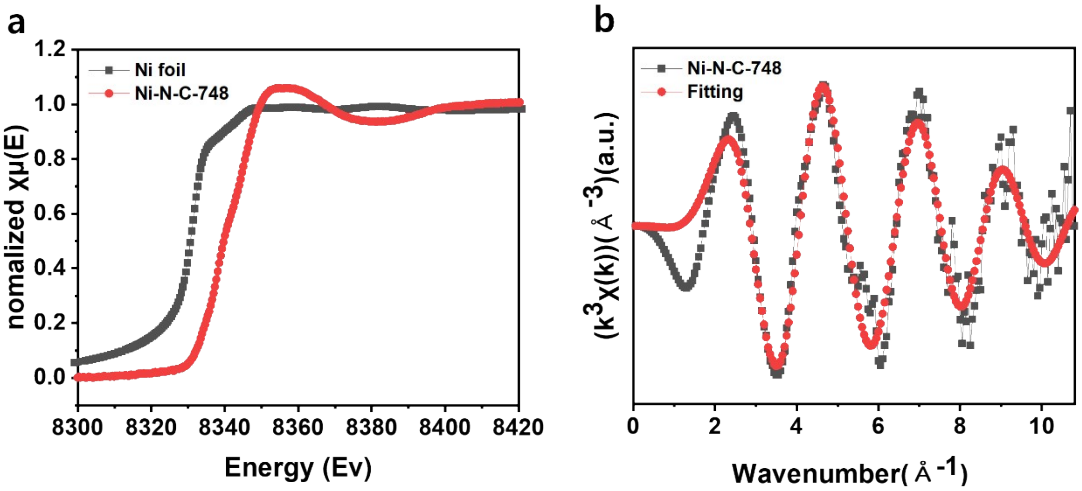

Fig. S6. a) XANES spectra of Ni-N-C 748 and Ni foil, b) the k-space EXAFS of Ni-N-C-748 at Ni K edge.

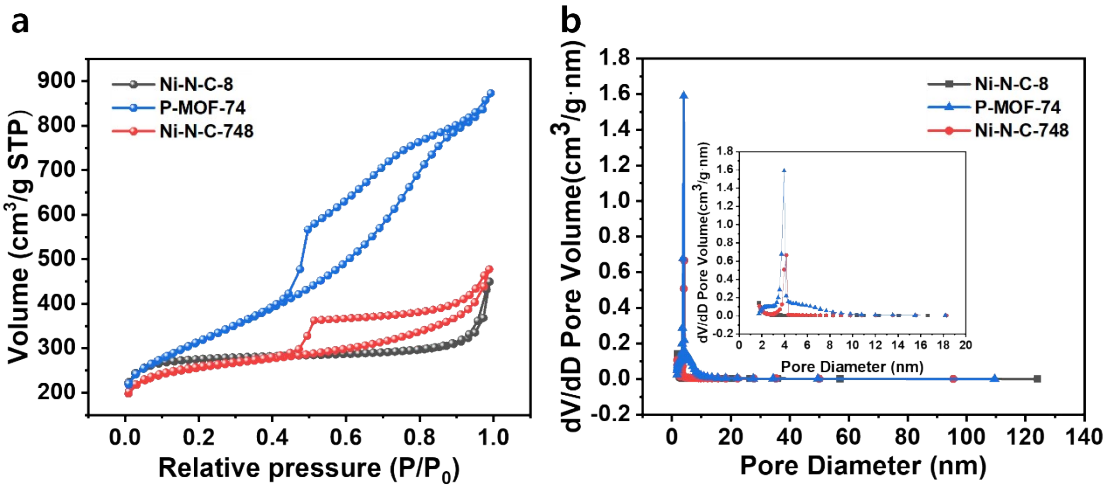

Fig. S7. a) The N_2 adsorption-desorption isotherms and pore size distributions of Ni-N-C-748, Ni-N-C-8 and P-MOF-74.

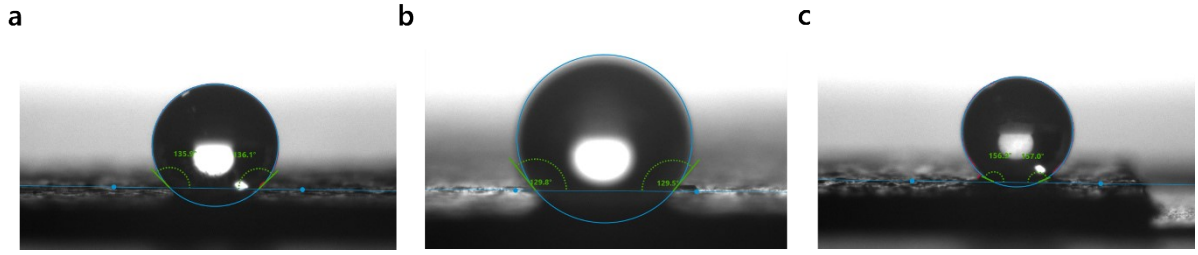

Fig. S8. Contact angle measurements of a) Ni-N-C-748, b) Ni-N-C-8 and c) P-MOF-74.

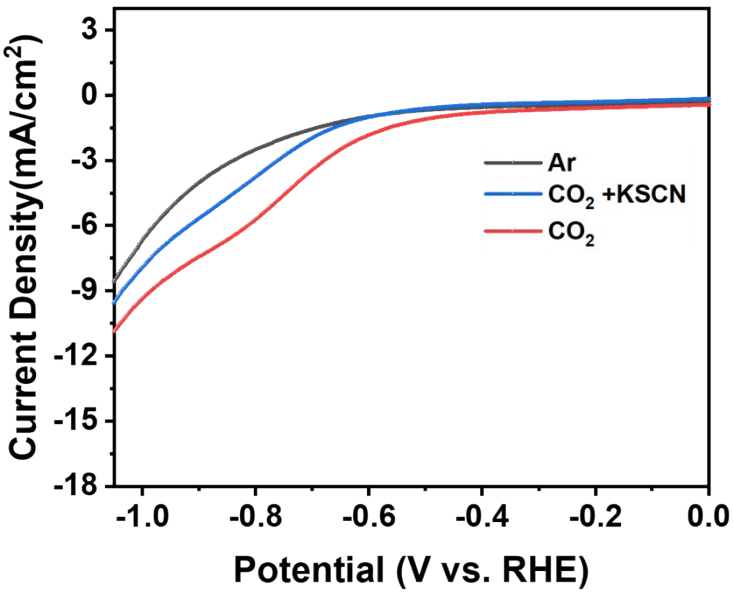

Fig. S9. LSV test in 0.5M $KHCO_3$ with purged Ar, CO_2 and CO_2 with $KHCO_3$.

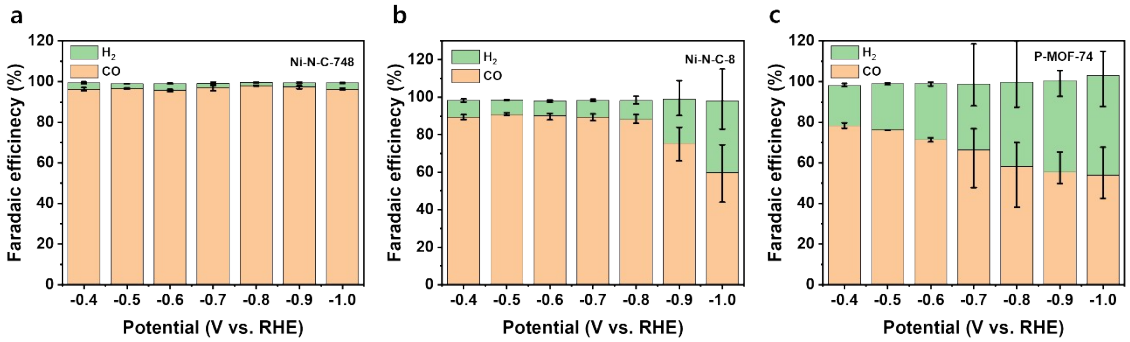

Fig. S10. F.E. of a) Ni-N-C-748, b) Ni-N-C-8 and c) P-MOF-74.

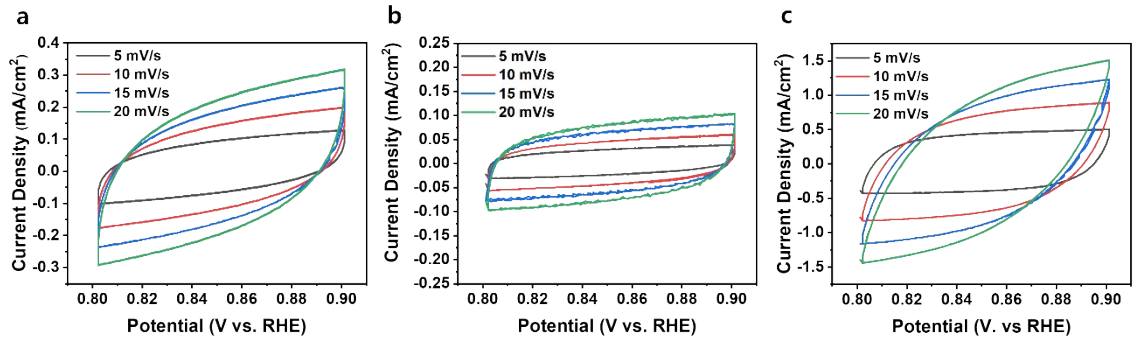

Fig. S11. ECSA test of a) Ni-N-C-748, b) Ni-N-C-8 and c) P-MOF-74.

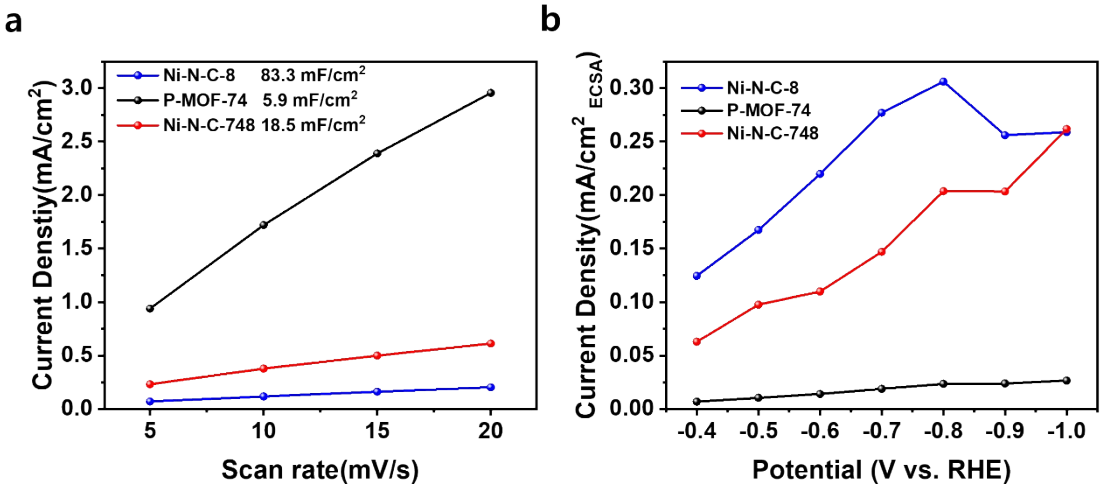

Fig. S12. a) ECSA capacitive current against scan rate and b) current density normalized with ECSA. ECSA result is as follows: Ni-N-C-748: 925.2 cm^2, Ni-N-C-8: 293.4 cm^2, P-MOF-74: 4167.4 cm^2.

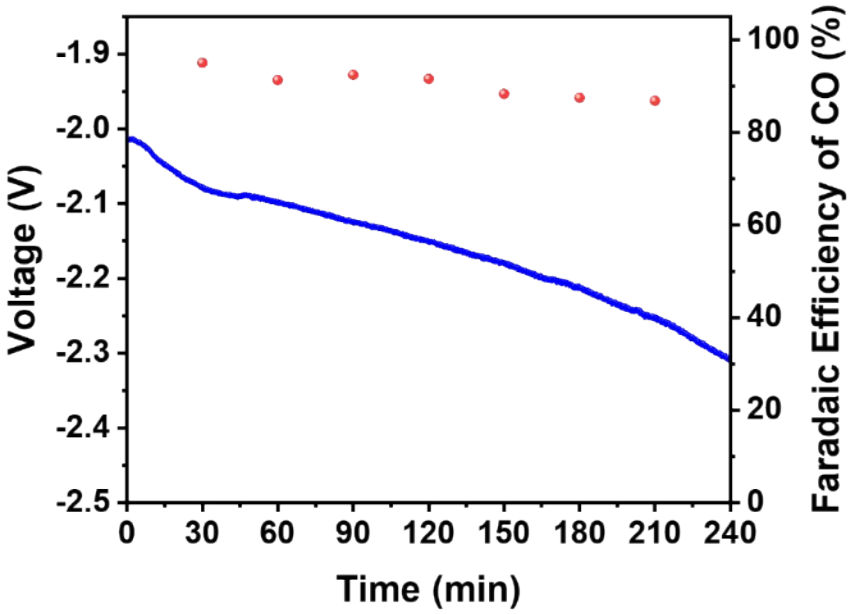

Fig. S13. Long-term stability test in the MEA cell without PTFE layer with humidified CO_2.

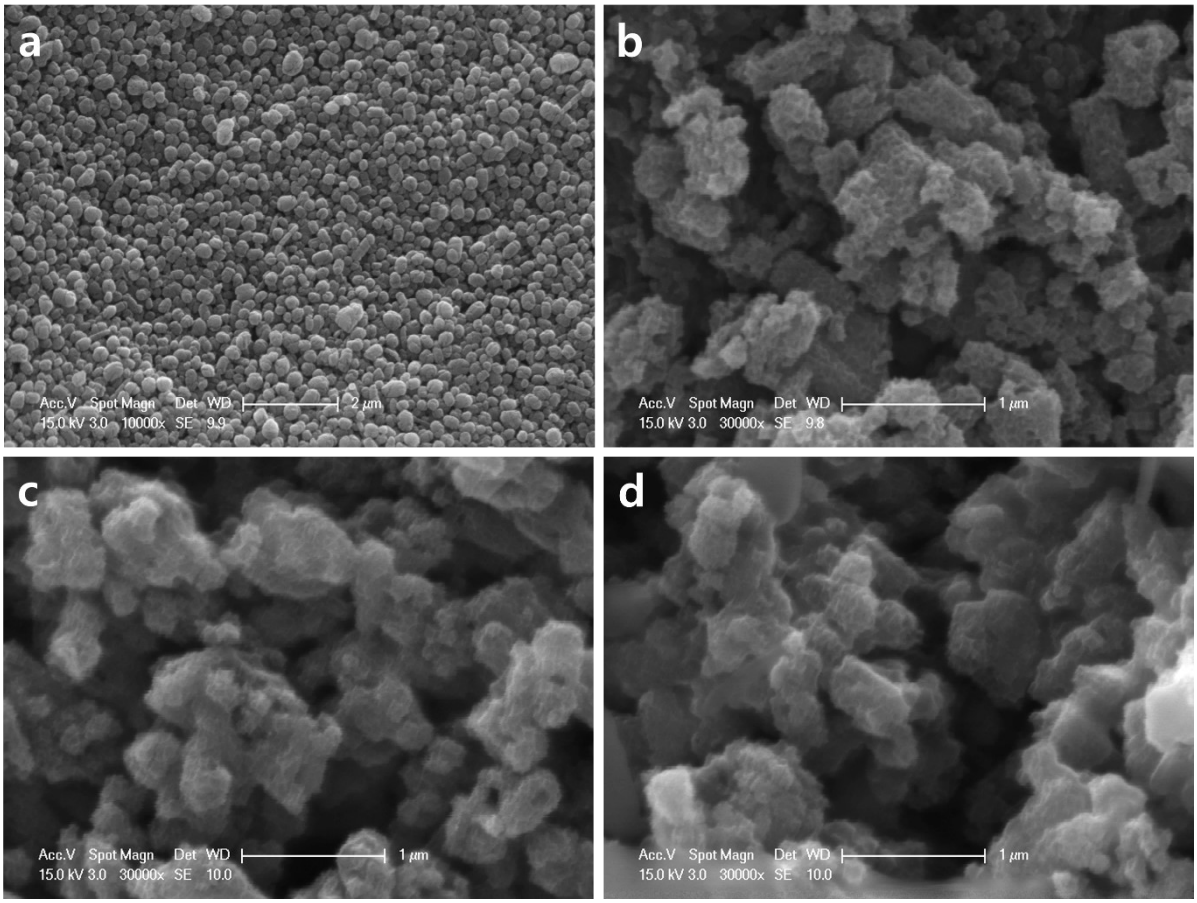

Fig. S14. SEM images of Ni-N-C-748 with PTFE layer a) before and b) after stability test. SEM images of Ni-N-C-748 without PTFE layer c) before and d) after stability test.

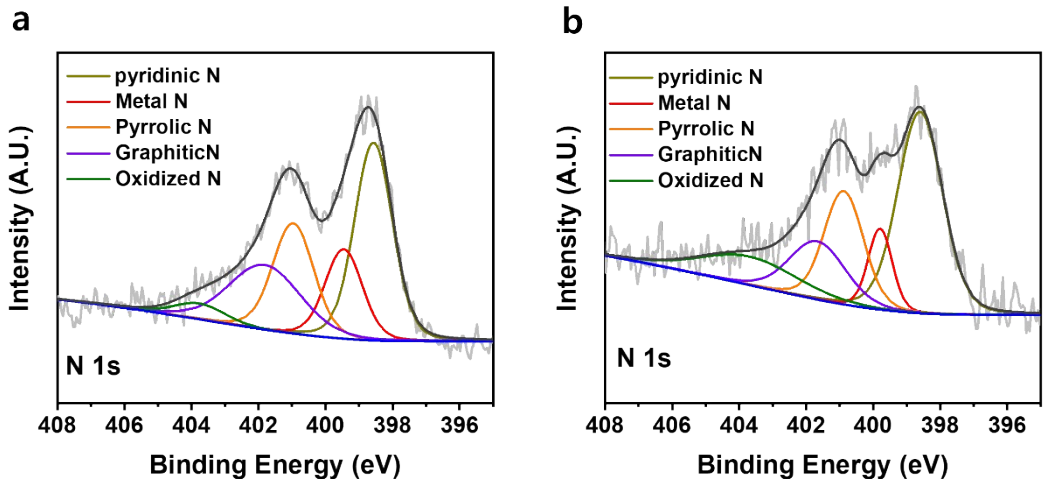

Fig. S15. N 1s XPS spectra of Ni-N-C-748 a) before and b) after stability test.

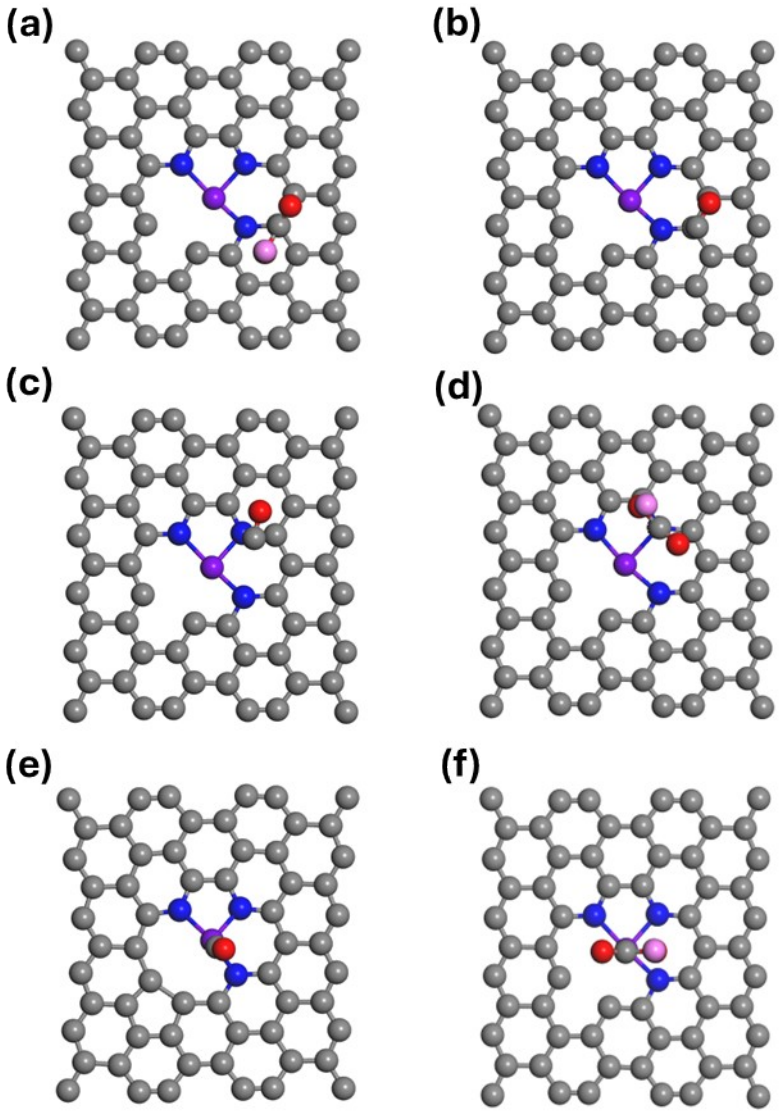

Fig. S16. Calculated DFT results for the adsorbed intermediates on different active sites on the surface of Ni-N_3C. The Figure shows a top view of the slab model for the adsorption of *COOH and *CO on the active sites of (a-b) C, (c-d) N, and (e-f) Ni, respectively. The following color scheme is used for the atoms: gray - C, blue - N, purple - Ni, red - O, and pink – H

Table S1. Parameters from fitting EXAFS at Ni K edge

CN: coordination number, R: bond distance, ΔE_0: edge energy correction, R factor: goodness of fitting, σ^2: Debye-Waller factor related with thermal and structural disorders.

S_0^2: amplitude reduction factor is obtained by Ni foil of EXAFS fitting reference.[7]

Catalyst	**Path**	**CN**	**R(Å)**	**ΔE_0**	σ^2	**R factor**
Ni-N-C-748	Ni-N	2.84	1.8655	-0.850	0.00982	0.00262

Table S2. The surface area and total pore volume of catalyst derived from N_2 adsorption/desorption isotherm

Catalyst	BET surface area (m^2/g)	Total pore volume (cm^3/g)
Ni-N-C-748	820.0844	0.738417
Ni-N-C-8	830.0983	1.350105
P-MOF-74	1077.1200	0.695266

Table S3. Calculated Gibbs free energy values for the catalytic systems

Catalyst	**Active site**	**Gibbs energy change (eV)**		
		ΔG_1	ΔG_2	ΔG_3
Ni-N_3-C	Ni	0.952	-1.456	0.712
	N	1.577	-0.678	-0.691
	C	1.922	-0.804	-0.910

References

1. G. Kresse and J. Furthmüller, Efficient iterative schemes for ab initio total-energy calculations using a plane-wave basis set, *Phys. Rev. B*, 1996, **54**, 11169-11186.
2. G. Kresse and J. Furthmüller, Efficiency of ab-initio total energy calculations for metals and semiconductors using a plane-wave basis set, *Computational Materials Science*, 1996, **6**, 15-50.
3. J. P. Perdew, M. Ernzerhof and K. Burke, Rationale for mixing exact exchange with density functional approximations, *Journal of Chemical Physics*, 1996, **105**, 9982-9985.
4. J. P. Perdew, K. Burke and M. Ernzerhof, Generalized Gradient Approximation Made Simple, *Phys. Rev. Lett.*, 1996, **77**, 3865-3868.
5. S. Grimme, Semiempirical GGA-type density functional constructed with a long-range dispersion correction, *Journal of computational chemistry*, 2006, **27**, 1787-1799.
6. H. A. Hansen, J. B. Varley, A. A. Peterson and J. K. Nørskov, Understanding trends in the electrocatalytic activity of metals and enzymes for CO2 reduction to CO, *Journal of Physical Chemistry Letters*, 2013, **4**, 388-392.
7. Y. E. Kim, Y. N. Ko, B. S. An, J. Hong, Y. E. Jeon, H. J. Kim, S. Lee, J. Lee and W. Lee, Atomically Dispersed Nickel Coordinated with Nitrogen on Carbon Nanotubes to Boost Electrochemical CO2 Reduction, *ACS Energy Letters*, 2023, **8**, 3288-3296.